Optimal Element Spacing for RIS-aided MIMO Terahertz Communication

Arnold Matemu*, Dong Ho Kim[†], and Kyungchun Lee*
Seoul National University of Science and Technology

* Department of Electrical and Information Engineering. Email: amatemu, kclee@seoultech.ac.kr

† Department of Smart ICT Convergence. Email: dongho.kim@seoultech.ac.kr

Abstract—In conventional multiple-input multiple-output (MIMO) systems, the antenna elements at the transmitter, receiver, and the reflecting elements at the reconfigurable intelligent surface (RIS) are typically spaced at $\lambda/2$ spacing. Such spacing often results in spatial correlation, which limits the multiplexing gain and, consequently, the achievable spectral efficiency. This limitation becomes more pronounced in the terahertz (THz) band, envisioned for future wireless systems, due to its severe propagation losses. To address this, we propose the design of the optimal element spacings that improve the multiplexing gain and spectral efficiency in RIS-aided THz MIMO communications. Simulation results show that the proposed design achieves significant gains over the conventional $\lambda/2$ spacing, demonstrating its potential for next-generation wireless networks.

Index Terms—Multiple-input multiple-output (MIMO), reconfigurable intelligent surface (RIS), multiplexing gain.

I. INTRODUCTION

With the continuous demand for high-speed connectivity and low-latency communication, ongoing research is exploring enabling technologies for future wireless networks. One promising direction is operation in the terahertz (THz) band, where abundant bandwidth is available [1]. However, THz propagation suffers from severe path loss, which limits the number of available multipaths and consequently reduces the spatial diversity that can be exploited [2]–[4].

Reconfigurable intelligent surfaces (RISs) have emerged as a promising solution to this limitation by enabling wireless environment reconfigurability and providing additional controllable propagation paths between the transmitter and receiver [1], [5]. Nevertheless, with the THz band inherently providing only a few propagation paths, even with RIS assistance, fully exploiting the available spatial degrees of freedom becomes critical, making multiplexing gain a key performance determinant.

In conventional point-to-point multiple-input multiple-output (MIMO) systems, where antenna elements are typically spaced at $\frac{\lambda}{2}$, with λ being the wavelength, the multiplexing gain is upper-bounded by $\min(L, N_T, N_R)$, where L is the number of available paths and N_T and N_R are the numbers of transmitter and receiver antenna elements, respectively [6].

This work was partly supported by the Institute of Information & communications Technology Planning & Evaluation (IITP) grant funded by the Korean government (MSIT) (No.RS-2023-00229330, 3D Digital Media Streaming Service Technology) and in part by the NRF grant funded by the Korean Government (MSIT) (RS-2025-21812978).

In the THz band, where L is inherently small due to high propagation loss, this bound becomes a major performance bottleneck.

Previous studies have explored different ways to improve multiplexing gain by optimizing antenna element spacing. For instance, [7] derived antenna separation spacing for achieving high-rank line-of-sight MIMO channels, while [8] demonstrated that maximum channel capacity can be achieved under specific distance—wavelength conditions. Moreover, [9] showed that employing a multi-subarray architecture with two distinct spacing levels enables two types of multiplexing gain in mmWave systems, which was later extended to the THz band in [10]. Despite these contributions, to the best of our knowledge, the optimal design of element spacing in RIS-aided MIMO systems for improving the multiplexing gain has not yet been addressed.

In this work, we investigate a point-to-point THz backhaul link assisted by an RIS. We derive the optimal element spacing that maximizes the multiplexing gain in RIS-aided MIMO systems and quantify the resulting performance improvements enabled by the proposed design. Our analysis, validated through simulations, reveals that in RIS-aided MIMO systems, the multiplexing gain can be improved specifically along the common axis of the transmitter, receiver, and RIS, contrary to conventional MIMO systems without RIS, where the multiplexing gain improvements can be achieved along both array axes.

II. SYSTEM MODEL

We study a downlink communication scenario assisted by RIS, where the transmitter, receiver, and RIS employ uniform planar arrays (UPAs). As illustrated in Fig. 1, the transmitter and receiver are arranged in the xz-plane with a separation distance $D^{R,T}$. The transmitter array contains N_{Tx} and N_{Tz} antenna elements along the x- and z-directions, respectively, yielding a total of $N_T = N_{Tx}N_{Tz}$ elements. Similarly, the receiver has N_{Rx} elements along the x-axis and N_{Rz} elements along the z-axis, yielding $N_R = N_{Rx}N_{Rz}$ total elements. The antenna elements at the transmitter and receiver are considered to be spaced by d_k^x and d_k^z along the x- and x-axes, respectively, where x- and x-axes, respectively, where x- are transmitter x- and x-axes, respectively.

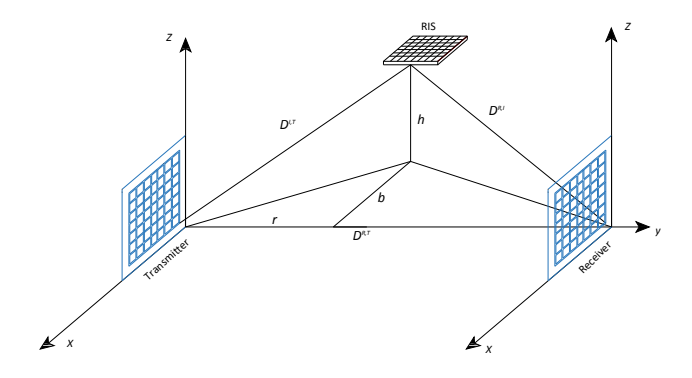


Fig. 1. System Model.

The RIS is assumed to be mounted parallel to the xy-plane at a height h relative to the transmitter and receiver. Its position is offset horizontally by b from the yz-plane and by r from the xz-plane. The RIS consists of N_{Ix} and N_{Iy} reflecting elements along the x- and y-axes, respectively, separated by d_I^x and d_I^y along the corresponding axes, yielding $N_I = N_{Ix}N_{Iy}$ total RIS elements.

III. ELEMENT SPACING ANALYSIS FOR MULTIPLEXING

We begin by examining the wireless channel between the nth transmit element and the mth RIS element, denoted as $G_{m,n}$. By using the principles of ray tracing, this channel is characterized by the corresponding path length $D_{(m,n)}^{(I,T)}$ and is expressed as [9]

$$G_{m,n} = \alpha e^{-j\frac{2\pi}{\lambda}D_{(m,n)}^{(I,T)}},$$
 (1)

where α is the path gain and λ is the wavelength.

We assume that the reference element in each array is the bottom right element, and that the reference element at the transmitter is located at the origin. Under this assumption, the position of the nth transmit element and the mth RIS element can be described as

$$\boldsymbol{a}_{T}^{n} = \begin{bmatrix} n_{x} d_{T}^{x} \\ 0 \\ n_{z} d_{T}^{z} \end{bmatrix}, \tag{2}$$

and

$$\boldsymbol{a}_{I}^{m} = D_{0,0}^{(I,T)} \begin{bmatrix} \sin \theta_{I} \cos \phi_{I} \\ \sin \theta_{I} \sin \phi_{I} \\ \cos \theta_{I} \end{bmatrix} + \begin{bmatrix} m_{x} d_{I}^{x} \\ m_{y} d_{I}^{y} \\ 0 \end{bmatrix}, \quad (3)$$

respectively, where $n_x = (n-1) \mod N_{T_x}$ and $m_x = (m-1) \mod N_{I_x}$ represents the x-indices of the nth transmit antenna and the mth RIS element, respectively, while $n_z = \lfloor \frac{(n-1)}{N_{T_x}} \rfloor$ and $m_y = \lfloor \frac{(m-1)}{N_{I_x}} \rfloor$ denote the z-index of the nth transmit antenna and the y-index of the mth RIS element, respectively. Furthermore, θ_I and ϕ_I denote the elevation and azimuth angles, respectively, of the RIS position, and

 $D_{0,0}^{(I,T)}=\sqrt{r^2+b^2+h^2}$ denotes the distance between the RIS reference antenna and the transmitter reference antenna. Following from (2) and (3), the distance $D_{(m,n)}^{(I,T)}$ can be computed as

$$\begin{split} D_{(m,n)}^{(I,T)} &= \|\boldsymbol{a}_{I}^{m} - \boldsymbol{a}_{T}^{n}\| \\ &= \left[\left(D_{0,0}^{(I,T)} \sin \theta_{I} \cos \phi_{I} + m_{x} d_{I}^{x} - n_{x} d_{T}^{x} \right)^{2} + \\ & \left(D_{0,0}^{(I,T)} \sin \theta_{I} \sin \phi_{I} + m_{y} d_{I}^{y} \right)^{2} + \\ & \left(D_{0,0}^{(I,T)} \cos \theta_{I} - n_{z} d_{T}^{z} \right)^{2} \right]^{\frac{1}{2}} \\ &\stackrel{\text{(a)}}{\approx} D_{0,0}^{(I,T)} + \left[\left(m_{x} d_{I}^{x} - n_{x} d_{T}^{x} \right) \sin \theta_{I} \cos \phi_{I} + \\ & m_{y} d_{I}^{y} \sin \theta_{I} \sin \phi_{I} - n_{z} d_{T}^{z} \cos \theta_{I} \right] + \\ & \frac{1}{2D_{0,0}^{(I,T)}} \left[\left(m_{x} d_{I}^{x} - n_{x} d_{T}^{x} \right)^{2} + \left(m_{y} d_{I}^{y} \right)^{2} + \left(n_{z} d_{T}^{z} \right)^{2} \right], \end{split}$$

where (a) follows from the second-order Taylor expansion approximation. Following from (4), the channel response from the nth transmit element to all N_I RIS elements can be expressed as

$$G_n = \alpha \left[e^{-j\frac{2\pi}{\lambda}D_{0,n}^{(I,T)}}, \dots, e^{-j\frac{2\pi}{\lambda}D_{(N_I-1),n}^{(I,T)}} \right]^T.$$
 (5)

By assuming $N_I > N_T$, achieving a full-rank G, which is essential for maximizing spectral efficiency, requires the columns of G to be linearly independent [11]. Orthogonality among the columns is a sufficient condition to ensure full rank, and in this work, we enforce orthogonality among the columns of G to guarantee that a full-rank matrix is achieved. Orthogonality can be enforced by ensuring that the inner product between the channel vectors corresponding to any two different transmit antennas is zero [7]. Based on (5), and considering the channel responses from the n_1 th and n_2 th transmit antennas to all N_I RIS elements, the inner product between the corresponding channel vectors is given by

$$\langle \boldsymbol{G}_{n_{1}}, \boldsymbol{G}_{n_{2}} \rangle = \boldsymbol{G}_{n_{1}}^{H} \boldsymbol{G}_{n_{2}}$$

$$= \sum_{m=0}^{N_{I}-1} \exp \left(\frac{j2\pi}{\lambda} \left(D_{(m,n_{1})}^{(I,T)} - D_{(m,n_{2})}^{(I,T)} \right) \right)$$

$$= c_{1} \sum_{m_{y}=0}^{N_{I_{y}}-1} \sum_{m_{x}=0}^{N_{I_{x}}-1} \exp \left(\frac{j2\pi}{\lambda} \frac{d_{I}^{x} d_{T}^{x}}{D_{0,0}^{(I,T)}} \left[m_{x} \left(n_{2_{x}} - n_{1_{x}} \right) \right] \right),$$
(6)

where

$$c_{1} = \exp\left(\frac{j2\pi}{\lambda} \left[(n_{2x} - n_{1x}) d_{T}^{x} \sin \theta_{I} \cos \phi_{I} + (n_{2z} - n_{1z}) d_{T}^{z} \cos \theta_{I} \right] \right)$$

$$\exp\left(\frac{j\pi}{\lambda D_{0,0}^{(I,T)}} \left[(n_{1x}^{2} - n_{2x}^{2}) d_{T}^{x^{2}} + (n_{1z}^{2} - n_{2z}^{2}) d_{T}^{z^{2}} \right] \right).$$
(7)

Furthermore, by using the definition of the geometric sun of complex exponentials [7], [12], (6) can be further simplified as

$$\langle G_{n_{1}}, G_{n_{2}} \rangle = c_{1} \sum_{m_{y}=0}^{N_{I_{y}}-1} \sum_{m_{x}=0}^{N_{I_{x}}-1} \exp \left(\frac{j2\pi}{\lambda} \frac{d_{I}^{x} d_{T}^{x}}{D_{0,0}^{(I,T)}} \left[m_{x} \left(n_{2_{x}} - n_{1_{x}} \right) \right] \right)$$

$$= c_{1} \sum_{m_{y}=0}^{N_{I_{y}}-1} \exp \left(\frac{j\pi}{\lambda} \frac{d_{I}^{x} d_{T}^{x}}{D_{0,0}^{(I,T)}} \left(N_{I_{x}} - 1 \right) \left(n_{2_{x}} - n_{1_{x}} \right) \right)$$

$$\frac{\sin \left(\frac{\pi}{\lambda} \frac{d_{I}^{x} d_{T}^{x}}{D_{0,0}^{(I,T)}} \left(n_{2_{x}} - n_{1_{x}} \right) N_{I_{x}} \right)}{\sin \left(\frac{\pi}{\lambda} \frac{d_{I}^{x} d_{T}^{x}}{D_{0,0}^{(I,T)}} \left(n_{2_{x}} - n_{1_{x}} \right) N_{I_{x}} \right)}$$

$$= c_{1} c_{2} N_{I_{y}} \frac{\sin \left(\frac{\pi}{\lambda} \frac{d_{I}^{x} d_{T}^{x}}{D_{0,0}^{(I,T)}} \left(n_{2_{x}} - n_{1_{x}} \right) N_{I_{x}} \right)}{\sin \left(\frac{\pi}{\lambda} \frac{d_{I}^{x} d_{T}^{x}}{D_{0,0}^{(I,T)}} \left(n_{2_{x}} - n_{1_{x}} \right) \right)},$$
(8)

where $c_2 = \exp\left(\frac{j\pi}{\lambda}\frac{d_I^xd_T^x}{D_{0,0}^{(I,T)}}\left(N_{I_x}-1\right)\left(n_{2_x}-n_{1_x}\right)\right)$. Following from (8), the inner product is equal to zero if and only the numerator is zero while the denominator remains nonzero. This condition can be satisfied by setting the product as

$$d_I^x d_T^x = \frac{\lambda D_{0,0}^{(I,T)}}{N_{I_x}}. (9)$$

A similar analysis can be carried out for the RIS-receive channel, \boldsymbol{H}_r , where, to improve the channel rank betwee these arrays, for a case when $N_I > N_R$, the antenna separatio product must be set as

$$d_R^x d_I^x = \frac{\lambda D_{0,0}^{(R,I)}}{N_I},\tag{16}$$

where $D_{0,0}^{(R,I)}=\sqrt{(D^{R,T}-r)^2+b^2+h^2}$ is the distance between the RIS reference element and the receiver reference element

Following the above analysis, the expressions in (9) and (10) suggest that in RIS-aided MIMO systems, orthogonality among the channels can be improved only along the direction that is common to all arrays, in this case, the *x*-axis. This behavior contrasts with conventional MIMO systems without RIS, where orthogonality can be achieved along both array axes. As a result, in RIS-assisted MIMO, it is more beneficial to employ uniform linear arrays (ULAs) aligned along the common axis of the transmitter, RIS, and receiver, rather than UPAs, since only the elements positioned along the shared direction contribute effectively to improving multiplexing gain.

IV. SIMULATION RESULTS

In this section, we present numerical results that validate the proposed analysis. Specifically, we evaluate the multiplexing gain under different configurations by computing the rank of the channel matrices for both the proposed element spacing and the conventional $\frac{\lambda}{2}$ spacing.

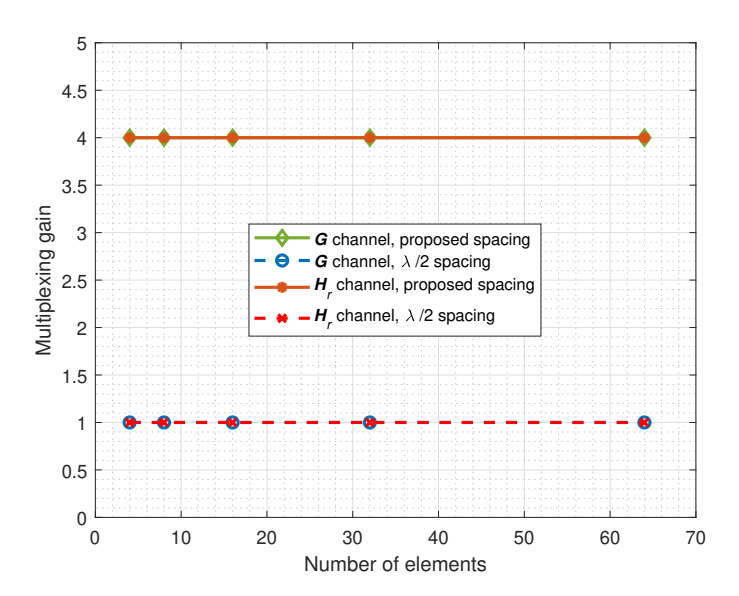


Fig. 2. Channel rank versus total number of elements.

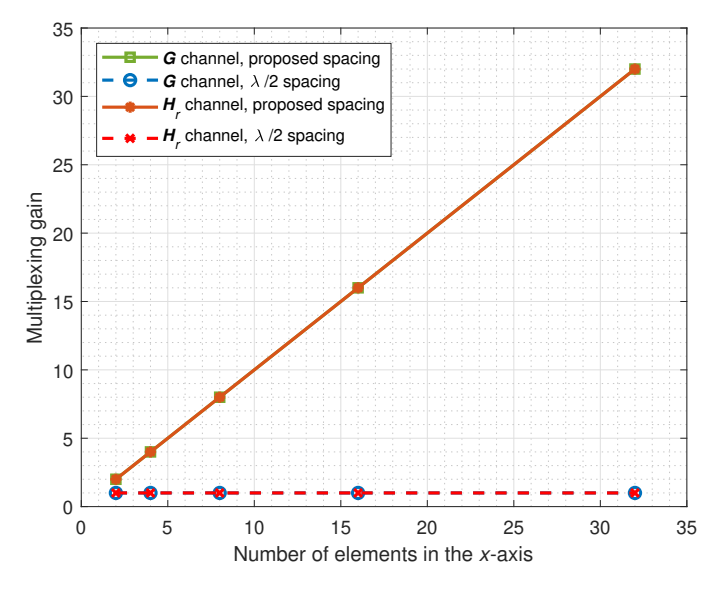


Fig. 3. Channel rank versus total number of elements in the x-axis.

Figs. 2 and 3 illustrate the effect of the number of elements on the multiplexing gain, when L=1. In Fig. 2, we vary the total number of elements such that $N_T=N_I=N_R=N$, while fixing the number of elements along the x-axis to $N_{T_x}=N_{I_x}=N_{R_x}=N_x=4$. The results show that the multiplexing gain achieved with the proposed spacing remains constant and equal to the number of x-axis elements, whereas with conventional $\frac{\lambda}{2}$ spacing, the gain is limited to the number of available paths.

In Fig. 3, we instead vary the number of elements along the x-axis while keeping the total number of elements fixed at 128. Here, we observe that, under the proposed spacing, the multiplexing gain increases with the number of x-axis elements, whereas it remains constant under conventional $\frac{\lambda}{2}$ spacing. These findings highlight a key distinction in RIS-aided systems, where the achievable multiplexing gain is

primarily determined by the number of elements aligned along the common axis, in contrast to conventional MIMO systems (without RIS), where gains can be improved by increasing elements in both dimensions.

V. Conclusion

In this work, we investigated a point-to-point THz backhaul link assisted by an RIS. We derived the optimal element spacing that maximizes the multiplexing gain in RIS-aided MIMO systems and quantified the resulting performance improvements. Our analysis and simulation results reveal that, unlike conventional MIMO systems, the multiplexing gain in RIS-assisted scenarios can be improved only along the common axis of the transmitter, RIS, and receiver. This finding highlights that employing ULAs aligned with the common axis is more advantageous than UPAs in RIS-aided systems. Overall, the proposed design demonstrates significant spectral efficiency gains compared to conventional $\frac{\lambda}{2}$ spacing, underscoring its potential to enable next-generation THz communications.

REFERENCES

- N. Rajatheva, I. Atzeni, E. Bjornson, A. Bourdoux, S. Buzzi, J.-B. Dore, S. Erkucuk, M. Fuentes, K. Guan, Y. Hu *et al.*, "White paper on broadband connectivity in 6G," *arXiv preprint arXiv:2004.14247*, 2020.
- [2] J. M. Jornet and I. F. Akyildiz, "Channel modeling and capacity analysis for electromagnetic wireless nanonetworks in the terahertz band," *IEEE Trans. Wireless Commun*, vol. 10, no. 10, pp. 3211–3221, 2011.
- [3] C. Han, A. O. Bicen, and I. F. Akyildiz, "Multi-ray channel modeling and wideband characterization for wireless communications in the terahertz band," *IEEE Trans. Wireless Commun*, vol. 14, no. 5, pp. 2402– 2412, 2015
- [4] C. Han and I. F. Akyildiz, "Three-dimensional end-to-end modeling and analysis for graphene-enabled terahertz band communications," *IEEE Trans. Veh. Technol.*, vol. 66, no. 7, pp. 5626–5634, 2017.
- [5] S. Zhang and R. Zhang, "Capacity characterization for intelligent reflecting surface aided MIMO communication," *IEEE J. Sel. Areas Commun.*, vol. 38, no. 8, pp. 1823–1838, 2020.
- [6] O. E. Ayach, S. Rajagopal, S. Abu-Surra, Z. Pi, and R. W. Heath, "Spatially sparse precoding in millimeter wave MIMO systems," *IEEE Trans. Wireless Commun.*, vol. 13, no. 3, pp. 1499–1513, 2014.
- [7] F. Bøhagen, P. Orten, and G. E. Øien, "Design of optimal high-rank line-of-sight MIMO channels," *IEEE Trans. Wireless Commun.*, vol. 6, no. 4, pp. 1420–1425, 2007.
- [8] P. Larsson, "Lattice array receiver and sender for spatially orthonormal MIMO communication," in 2005 IEEE 61st Vehicular Technology Conference, vol. 1, 2005, pp. 192–196 Vol. 1.
- [9] X. Song, W. Rave, N. Babu, S. Majhi, and G. Fettweis, "Two-level spatial multiplexing using hybrid beamforming for millimeter-wave backhaul," *IEEE Trans. Wireless Commun*, vol. 17, no. 7, pp. 4830– 4844, 2018.
- [10] L. Yan, Y. Chen, C. Han, and J. Yuan, "Joint inter-path and intrapath multiplexing for terahertz widely-spaced multi-subarray hybrid beamforming systems," *IEEE Trans. Commun.*, vol. 70, no. 2, pp. 1391– 1406, 2021.
- [11] D. G. Zill, Advanced engineering mathematics. Jones & Bartlett Learning, 2020.
- [12] L. Råde and B. Westergren, Mathematics handbook for science and engineering. Springer, 2004.